Field scale interaction and nutrient exchange between surface water and shallow groundwater in the Baiyang Lake region, North China Plain

Brauns, Bentje; Bjerg, Poul Løgstrup; Song, Xianfang; Jakobsen, Rasmus

Published in:
Journal of Environmental Sciences

Link to article, DOI:
10.1016/j.jes.2015.11.021

Publication date:
2016

Document Version
Peer reviewed version

Field scale interaction and nutrient exchange between surface water and shallow groundwater in the Baiyang Lake region, North China Plain

Bentje Brauns[1,2,3,*], Poul L. Bjerg1, Xianfang Song[2] and Rasmus Jakobsen[4]

[1]Department of Environmental Engineering, Technical University of Denmark, Kongens Lyngby, Denmark.

[2]Key Laboratory of Water Cycle and Related Land Surface Processes, Institute of Geographic Sciences and Natural Resources Research, Chinese Academy of Sciences, Beijing, China.

[3]Sino-Danish Center for Education and Research, Aarhus C, Denmark.

[4]Geological Survey of Denmark and Greenland, Copenhagen, Denmark.

E-Mail*: benb@env.dtu.dk

Abstract

Fertilizer input for agricultural food production, as well as domestic and industrial surface water pollutants in the North China Plain, increase pressures on locally scarce and vulnerable water resources. In order to: (a) understand pollutant exchange between surface water and groundwater, (b) quantify nutrient loadings, and (c) identify major nutrient removal pathways by using qualitative and quantitative methods, including the geochemical model PHREEQC, a one-year study at a wheat (*Triticum aestivum L.*) and maize (*Zea mays L.*) double cropping system in the Baiyang Lake area in Hebei Province, China, was undertaken. The study showed a high influence of low-quality surface water on the shallow aquifer. Major inflowing pollutants into the aquifer were ammonium and nitrate via inflow from the adjacent Fu River (up to 29.8 mg/L NH_4-N and 6.8 mg/l NO_3-N), as well as nitrate via vertical transport from the field surface (up to 134.8 mg/L NO_3-N in soil water). Results from a conceptual model show an excess nitrogen input of about 320 kg/ha/a. Nevertheless, both nitrogen species were only detected at low concentrations in shallow groundwater, averaging at 3.6 mg/L NH_4-N and 1.8 mg/L NO_3-N.

Measurement results supported by PHREEQC-modelling indicated cation exchange, denitrification, and anaerobic ammonium oxidation coupled with partial denitrification as major nitrogen removal pathways. Despite this current removal capacity, the excessive nitrogen fertilization may pose a future threat to groundwater quality. Surface water quality improvements are therefore recommended in conjunction with simultaneous monitoring of nitrate in the aquifer, and reduced agricultural N-inputs should be considered.

1 Introduction

Water pollution by nitrogen fertilizers has been recognized as a common environmental impact of agricultural activities in many regions (Costa et al., 2002; Rupert, 2008; Strebel et al., 1989; Zhang et al., 1996). However, as the world is facing demands for food that are estimated to increase by up to 70% by 2050 (Nelson, 2010), production - and therewith fertilization -must be kept high. To protect the equally important water resources, concurrent environmental monitoring and management of the local surface waters and aquifers become crucial. Because pollution sources and pathways in agricultural systems can show large spatial variability, knowledge of regional features and field scale interactions is an important area of research that gives base for the development of appropriate monitoring strategies—and the necessary protection measures.

China is the largest producer of grain worldwide, and has undergone large agricultural yield improvements for the three main staple foods (wheat, maize, and rice) in recent decades. In this way, the government's explicit goal to keep at least close to self-reliant in food has been fulfilled, despite the fact that it has to feed 20% of the world's population while relying on only 8% of the world's arable land. One of the most important production areas in the country is the North China Plain (NCP), which encompasses the north-eastern provinces of Beijing, Hebei, Shanxi, Shandong, and parts of Henan. The dominant agricultural production system in the NCP is a rotation of irrigated winter wheat (*Triticum aestivum L.*) and rainfed maize (*Zea mays L.*), of which the NCP produced 61% (wheat) and 39% (maize) of China's national output in 2012 (Zhao and Guo, 2013). Current enhancements in the productivity of the NCP have been driven by two major management changes: the expanded use of inorganic fertilizer since the 1970s, and the increase in irrigation (Li et al., 2011) that enables the harvest of two crops per year. However, the growth in production is taking a toll on the environment, and recent studies report overexploitation of local water resources with observed groundwater (GW) level declines of up to 1 m per year (Liu et al., 2008), as well as elevated nitrate concentrations in groundwaters exceeding 11.3 mg NO_3-N/L (50 mg NO_3/L), which is the World Health Organization's drinking water standard (Chen et al., 2005; Ju et al., 2006; Zhang et al., 1996).

In light of the increased water pollution, there is an urgent need to understand regional pollutant transport and removal, and to protect the local water resources in the NCP. In fact, numerous studies on best practices for crop management, irrigation management, and optimal fertilizer application have recently been published (Dikgwatlhe et al., 2014; Li et al., 2015; Sheldrick et al., 2003). Few studies also discussed the nutrient transport of polluted river water (RW) into wetland areas and lakes, and its potential impact on the ecosystem (Mao and Yang, 2011; Muqi et al., 1998; Wang et al., 2001). Others focused on nitrogen budgets (Liu et al., 2003; Zhao et al., 2006), or selected removal mechanisms such as anaerobic ammonium oxidation (anammox) (Zhu et al., 2013). However, little focus has been given to interactions and pollutant exchange between agriculture, RW, and GW, and to removal processes within the systems.

To fill this gap, the field study presented here was carried out on a typical wheat-maize field in the NCP near Baiyang Lake that is located directly adjacent to a passing stream (Fu River). Based on irrigation, crop management, and nutrient input, the objectives were to: (a) describe the local flow dynamics and solute transport between GW and RW, (b) assess temporal water quality changes in the GW regarding inorganic water chemistry and nitrogen, and (c) evaluate dominant geochemical processes, in particular nitrification/denitrification processes, by using qualitative and quantitative methods, including the geochemical modelling code PHREEQC. The insight and better understanding of the nitrogen sources, pathways, and removal processes in the RW-GW system enables us to develop a conceptual model for the nitrogen fluxes, and to reflect on future developments in nitrogen species and monitoring needs in the study area.

2 Materials and methods

2.1 Study area

The study was conducted on an agricultural site in Baoding County, Hebei Province, China, (38° 53' N, 115° 52' E) near the Baiyang Lake area and directly adjacent to Fu River, the lake's largest incoming stream (Figure 1). The study site is located in the agricultural area at the northern bank of Fu River near Dongxiangyang Village, which has about 5000 inhabitants. The parent material of the soil at the field site, which lies in the Hai River floodplain, is a quaternary re-deposited loess alluvium. The hydrogeological setting of the plain has been described as an unconfined shallow aquifer system, with an average water table depth of 20 m below surface in the plain area of the Baiyang catchment (Yuan et al., 2012). Even though GW levels in the NCP have been lowering in general, the ambient area around Baiyang Lake shows shallow depths, often less than 10 m below ground level.

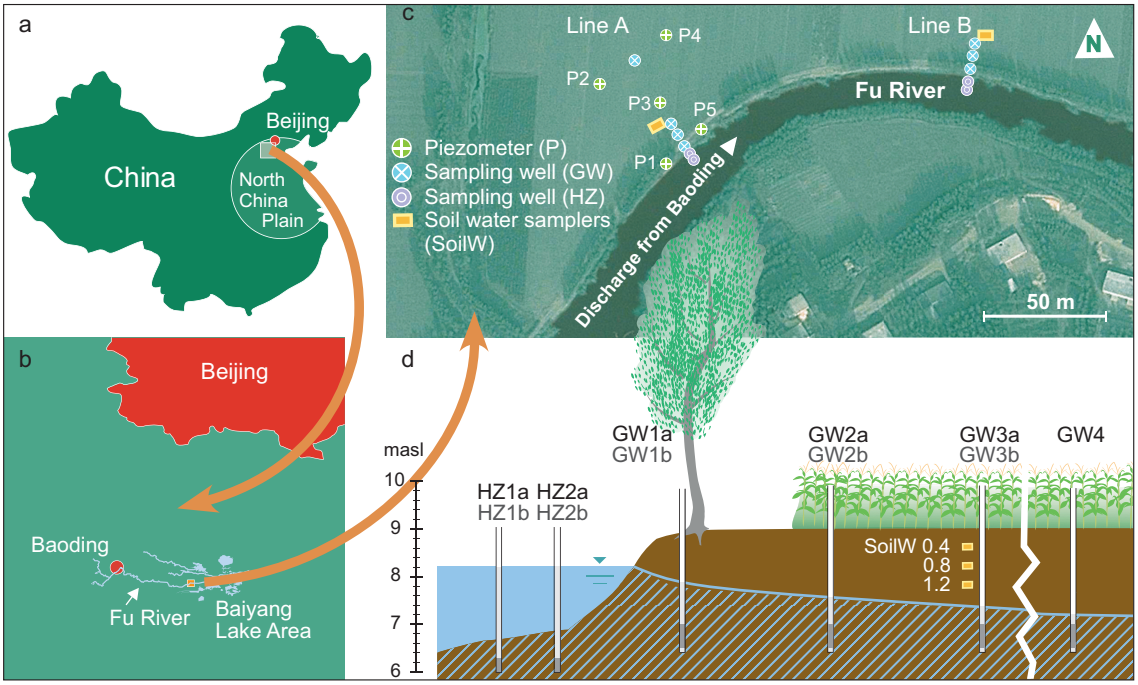

Figure 1. (a,b) Location of the field site, (c) aerial view of the sampling line A and B, and (d) cross-section of the installed wells and soil water samplers (labelling for sampling line A and B in black and in grey letters, respectively).

Fu River springs near Baoding City, and it is reported that it has little to no remaining natural headstream throughout most of the year, so it is nowadays primarily fed by industrial and untreated urban effluents (Muqi et al., 1998; Qiu et al., 2009). The RW quality is very poor, and Fu River has been classified as inferior to Grade V (unfit for direct human contact) in the 2013 Report on the State of the Environment in China (MEP, 2014). It has also been identified as one of the major causes for the water quality deterioration of Baiyang Lake (Muqi et al., 1998). However, little information can be found about the interaction between Fu River and the local GW resources.

2.2 Field site and crop management

The study area consists of several fields with different ownerships—a common characteristic in China caused by laws that regulate the distribution of small patches of land amongst the local population. The fields extend very close to the adjacent Fu River, with distances between the agricultural area and the river bank of only 5 to 10 m. Due to the relatively small size of each patch (about one hectare), farmers from adjacent fields usually cultivate the same crops and share the same schedule of seeding and harvesting. The field site is used without lag periods for the described winter wheat-summer maize double cropping system (which is typical for the NCP) and is managed according to local traditions. The winter wheat-summer maize rotation of the study year encompassed the growing season for wheat from October 2012 to June 2013, and that of maize from June to October 2013. Harvesting of the winter wheat was mechanized, whereas maize was harvested by hand. Remaining wheat stubbles were tilled under addition of inorganic fertilizer, and maize seeds were immediately planted. After the harvest of the maize, stems normally are first chopped, and then a rotary hoe is used to mix the remains and fertilizer, which prepares the land for the seeding of the winter wheat. In the study period 2013 to 2014, the field site was in danger of flooding during the autumn due to unusually high summer rainfalls, and the farmers refrained from planting winter wheat. Therefore, the maize stubs remained on the field, and the land became fallow during the remaining period of the study. Irrigation took place during the growing period of the wheat only (see Table 1 for more information on seeding/harvest times, irrigation, and fertilizer application).

Table 1. Planting times, irrigation, and fertilizer application during wheat and maize cultivation in 2012/2013.

	Date	Planting times		Irrigation	Fertilizer application			
		Seeding	Harvest	Applied amount (mm)	Type of fertilizer	Applied amount (kg ha^{-1})		
						N	P	K
Wheat	10 Oct 2012	+			Diammonium phosphate[1]	67	75	0
	11 Apr 2013				Urea[2]	192	0	0
	12 Apr 2013			40				
	1 May 2013			50				
	30 May 2013			60				
	10 Jun 2013		+					
Maize	12 Jun 2013	+			Compound fertilizer	149	31	40
	05 Oct 2013		+					
Total Oct'12-Oct'13			150	408		408	106	40
Total 2013			150	341		341	31	40

[1] $(NH_4)_2HPO_4$, [2] (CH_4N_2O)

2.3 Field data and sampling

Hydraulic heads of RW and GW were observed via automatic manometers (Mini and Micro Diver, Schlumberger, Netherlands) that were installed in five piezometers (P1-P5, see Figure 1) in the field and at one location in the river. Additional manual hydraulic head measurements were taken at each sampling campaign from the piezometers, as well as from the sampling wells. To obtain an estimate on vertical and horizontal subsurface water velocities, 6 moles of LiBr (dissolved in 10 L of water) were applied to the soil surface near sampling wells M3a and M3b on 25 April 2013. Based on after which sampling campaign the bromide (which functioned as unreactive tracer with no environmental background value) was detected in samples from soil water (SoilW) and GW, a range of potential velocities was calculated as estimates of the vertical and horizontal movement of water in the soil system. For determination of particle size distribution, total carbon (TC_s), total organic carbon (TOC_s), and total inorganic carbon (TIC_s) of the sediment, soil samples over a depth from 0–260 cm were taken via auger drilling from three locations within the agricultural field. Additionally, one sample over a depth from 0–50 cm was obtained from the hyporheic zone (HZ) during well installation during winter 2012/2013. The soil samples were segmented into the top 20 cm, and afterwards into intervals of 40 cm (the sample from the HZ was segmented into 0–20 and 20–50 cm).

Water sampling included 10 field campaigns at intervals of 20–57 days from March 2013 to March 2014. Samples were taken from RW, from the HZ below the river bed, and from GW wells along two sampling lines (Line A and Line B), with a screened depth of 1.9–2.4 m below the field surface (see Figures 1c and 1d). The distance of the GW wells from the river was 1, 6, and

11 m at both lines, and an additional well at a distance of 41 m was installed on Line A. For SoilW sampling, PTFE/quartz suction cups (Prenart Super Quartz Mini, Prenart Equipment ApS, Denmark) were placed at 0.4, 0.8, and 1.2 m depth and 11 m from the river. All water samples for ion analysis and isotopic measurements were collected using a low-flow peristaltic pump (~200mL/min), to which a flow cell was attached. The sampled water was filtered immediately through a 0.45 µm cellulose-ester membrane into three 20 ml polyethylene bottles, which were filled to overflowing and capped. The samples for cation analysis were acidified immediately (pH=2) using concentrated HNO_3. All samples were transported and stored at 4°C. Due to flooding issues in the second half of the year, SoilW could only be sampled from April to September 2013.

2.4 Soil and water analysis

Soil texture was analyzed using a particle-size analyzer (Analysette 22, Fritsch GmbH, Germany). TC_s was measured via elemental carbon analyzer (CS 200, LECO Corporation, USA), and the TOC_s was determined via the Walkley-Black method (Lettens et al., 2007). TIC_s was then calculated by subtracting TOC_s from TC_s. Water samples were measured in situ via electrodes in a flow cell for temperature (T), dissolved oxygen (DO), pH, and electrical conductivity (EC) with a field meter (Multi 3430, WTW, Germany), and alkalinity was determined via immediate titration in the field. NH_4-N was analyzed using a discrete analyzer (Smartchem 300, AMS Alliance, Italy), and all other cation analysis was done via ICP-OES (Optima 5300DV, PerkinElmer, USA). For the analysis of anions, an integrated IC System (ICS-2100, Thermo Scientific™, USA) was used and for δD and δ18O, an Isotope Ratio Mass Spectrometer (MAT 253, Thermo Scientific™, USA). The charge balance error for each of the 114 water samples was calculated and found to be within the permissible limit of ±5%.

2.5 Further geochemical analysis and modelling of inorganic chemistry

For further geochemical analysis of the water samples, saturation indices (SI) for different mineral phases and partial pressure of carbon dioxide (P_{CO_2}) were calculated using the geochemical speciation and modelling code PHREEQC Version 3 (Parkhurst and Appelo, 2013). Data input included T, DO, pH, alkalinity, and dissolved concentrations of the measured cations and anions. In addition to the speciation calculation, a 1-D horizontal transport

model in PHREEQC was used to simulate hydrogeochemical effects of the RW flowing into the aquifer. The model was set up to reflect water chemistry changes as well as changes on the exchanger sites (the soil) from March 2013 to September 2013. Different processes such as cation exchange (CE), equilibrium for calcite, carbon dioxide (simulating degassing of CO_2 from the extremely shallow water table) and iron(II) sulfide, degradation of organic matter (OM), redox processes, de-/nitrification, and anaerobic ammonium oxidation (anammox) were combined in different setups to identify the dominating removal processes for nitrogen and other ions (see Appendix A Table S1 for information on main input parameters). The model consisted of 42 cells, which each represent 1 m. The initial input to the first cell was a calculated average composition of the river water (RW_{avg}), which would then consecutively flush through the remaining model cells. The exchanger in all 42 model cells was initially equilibrated with and surrounded by the average annual groundwater sample composition on GW3, representing a type of "pristine" GW. To simulate pre-existing RW inflow before the field sampling campaign, RW_{avg} was first set to flush the soil for 18 months with the average flow velocity estimated from the tracer application experiment. After this initial step, RW compositions from each sampling campaign between March and July 2013 were used as input for cell 1, and would be allowed to propagate through the system for the equivalent timeframe until the next sampling date. Model results were compared to measured values from both sampling lines at the end of the respective time step.

To test for different removal pathways of nitrogen species, three different model setups were used. The first model (CE Model) simulated CE only, while the second model (CE-Calc Model) included CE, and calcite equilibrium. In both of these two models, ammonium was removed by CE. The third model (CE-Equil-OM-Anammox Model) combined CE, calcite equilibrium, OM (organic matter) degradation in the HZ, and– to a lesser degree– in GW, and an input of nitrate as electron acceptor. This input reflected vertical leaching of fertilizers that had been applied on the soil surface, and enabled the inclusion of the anammox process. Low amounts of oxygen input were added to reflect oxygen input from the unsaturated zone. As a tool for forward modelling, one cell (cell 42, representing sampling point GW4) of the best-fitting model was selected, at which all parameters (pH, alkalinity, and selected ions) were plotted over the simulated time of the model run to show the influence of the changing RW composition over time.

3 Results and discussion

3.1 Climate

The general climate of the region belongs to the temperate, semi-humid, monsoon zone and had a mean annual precipitation of 500 mm in 2003-2012, at a mean temperature of 13.4˚C (data according to Baoding Weather Station). Almost all of the annual rainfall occurs from June to September (about 80%), whereas there is little precipitation at other times of the year. During the study year (2013) and the previous year (2012), annual rainfall exceeded the 10-year average by 21% and 18%, respectively. Particularly strong rainfalls were observed from June-August 2013, which surpassed the 10-year average for these months by 57% (see Figure 2). Due to these unusually high rainfalls, and possibly further amplified by upstream flood divergence, the field site became flooded towards the end of the sampling period.

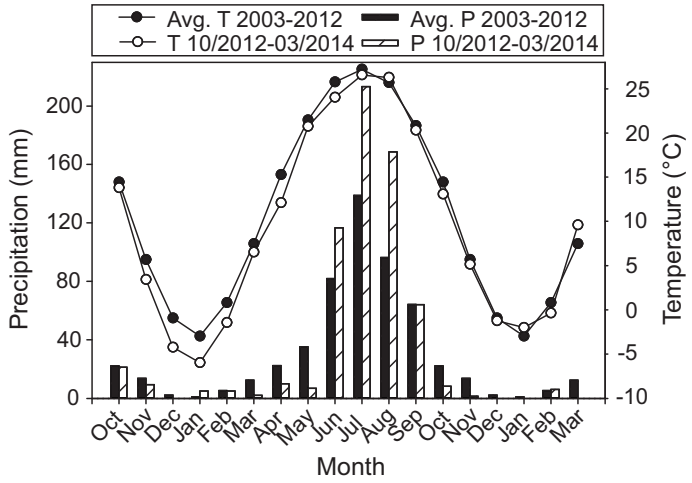

Figure 2. Average monthly temperature (T) and precipitation (P) as 10-year average (2003-2012) compared to the period from October 2012 to March 2013.

3.2 Water flow

GW levels ranged from about 1.7 m below the surface in June 2013, and rose to almost ground level from November 2013 onward (when the flooding occurred). In general, the RW level clearly exceeded GW levels. The only exceptions to this were the last months of the study, during which RW and GW levels were almost equal. However, even during this time, the flow direction did not reverse, so that similar conditions to before were still present. The hydraulic heads decreased from the river towards the sampling wells furthest into the field (see Figure 3). This indicates water flow from the

river into the field and minor flow from the Eastern into the Western part of the field, where a drainage ditch is located approximately 70 m from the closest sampling wells. The hydraulic gradient into the field was about 0.01 m/m (10 per mille) before the rainy season, and dropped to lower values after the first heavy rainfalls in June 2013. However, even after the unusual flooding of the site, no indications were found that GW might discharge into the river.

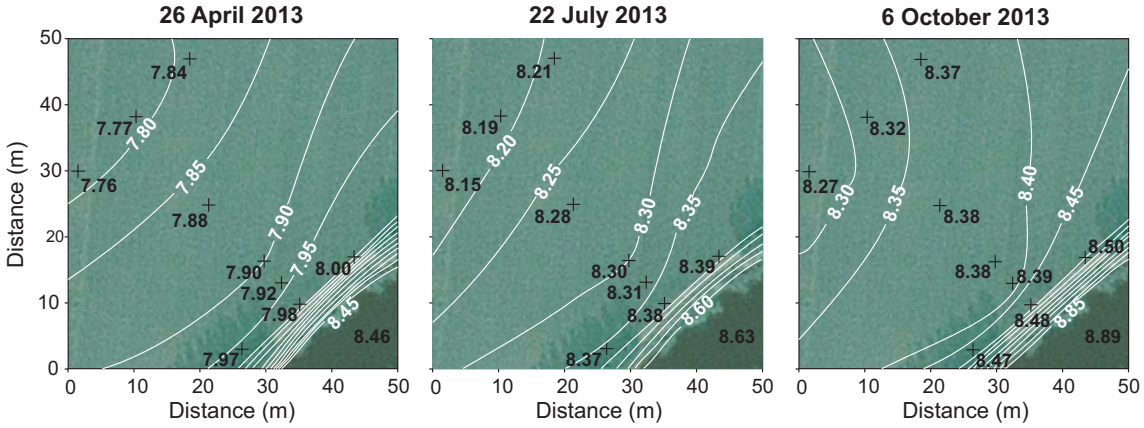

Figure 3. Hydraulic heads of the river and groundwater (P1-P5, see Figure 1 for detailed set-up) in April, July, and October 2013 and isopotential lines.

Temperatures within the piezometers and sampling wells were decreasing from the river inland from March-September 2013 (when the RW was very warm), and a reverse trend could be observed during the remaining months of the year. This indicates that the RW is influencing the GW temperatures, and therefore confirms that the river is recharging the lower aquifer. The LiBr-tracer (applied in April 2013) was detected at the upper SoilW samplers SoilWa-0.4 and SoilWb-0.4 during the field campaigns in May and July 2013, respectively, and at the water table (at that time 65 cm below the surface) after the first heavy summer rainfalls at the end of July. The first detection of bromide in the GW samples from the screened depth of 1.9-2.4 m occurred in November 2013 at GW3a, and in January 2014 at GW3b—correlating to 200 and 250 days after application, respectively. The additional sampling well GW4 (41 m from the river edge) showed increased bromide levels after another 80 days. This propagation of the bromide tracer from GW3a to GW4 further confirmed the suspected flow from Fu River to the field, as indicated by the hydraulic head measurements and the temperature gradient. Based on the bromide tracer measurements, vertical water flow from the field surface to SoilW 1.2 seemed to be in the range of 1.4-3.3 cm/day. The flow from GW3a to GW4 was about 0.2-0.7 m/day. This was 4-

5 orders of magnitude higher than the velocity calculated with HydrogeoSieveXL, which is based on grain size distribution (Devlin, 2015), and indicates that flow through macropores must be occurring. The δ18O and δ2H values of the water samples showed relatively large fluctuations throughout the year. They ranged from -8.3 to -5.2 ‰ and from -62.1 to -46.2 ‰, respectively. The similarity of the isotopic ratios between RW and GW was slightly higher for GW samples from close to the river than for samples further away from the river. Additionally, the ratios from floodwater on the field and GW showed some similarities. These similarities, the water level measurements, the temperature gradient between RW and GW, and the transport of the bromide tracer from GW3a to GW4 show that RW is discharging into the GW.

Generally, it therefore seems certain that RW and GW are well connected throughout the year, and that the two water bodies mix. Since the RW flows into the shallow aquifer, it may transport contaminants into the GW. The extreme shallowness of the GW means that contaminants prone to leaching, such as nitrate fertilizer that is applied on the field surface, have a short travel time to the saturated zone, and therefore might easily cause GW pollution.

3.3 Soil properties

The soil consists of silty clay loam and shows a very homogenous particle size distribution across the analyzed depth profile from 0-240 cm (0-50 cm for the sample from the HZ), and across the four sampling locations themselves (Figure 4).

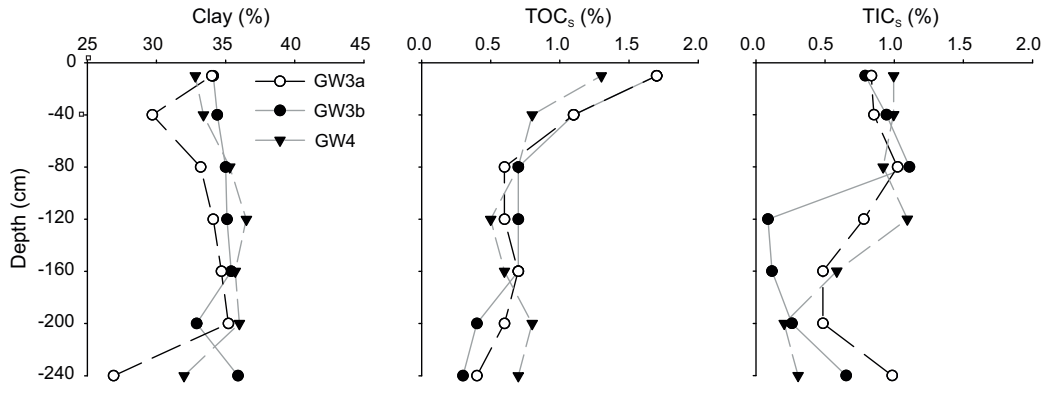

Figure 4. Clay content, total organic soil carbon (TOC_s) and total inorganic soil carbon (TIC_s) in percent of dry weight from soil samples near GW3a, GW3b and GW4 (see Figure 1 for location of the sampling points). Calculations are based on particle-size analysis, Walkley-Black titration for TOC, and elemental carbon analysis for determination of total carbon (TIC = total carbon – TOC).

The highest clay content of the samples was 36%, and none of the samples contained particles larger than 0.03 mm. The profiles for the sampling points GW3a and GW4 have a very similar pattern with slightly decreasing clay content at 2.4 m depth, while the clay fraction at GW3b does not change as much over depth. TOC_s within the topsoil of the field ranged from 1.3-1.7%, and generally decreased with depth, though two of the analyzed soil profiles showed local increases from 1.0-1.8 m depth (Figure 4). This was in accordance with visual observations (slightly darker, oozy material was observed at this depth) during sample-taking. TIC_s ranged from 0.2-1.1% and there was a decline between 80 and 200 cm depth, after which it increased again at 240 cm depth.

Overall, the values of 1.3-1.7% TOC_s in the top layer are within the desired range for agricultural soils, and show the suitability of the soil for agricultural practice. The homogenous silty clay loam texture provides for a high water holding capacity and high cation exchange capacity, due to the high clay content. Both are desirable features to prevent nutrient leaching. The decline in TIC_s correlates with the depth at which normal water table fluctuations for this site were expected, and one explanation could be that hydrogen ion producing processes (such as ammonium oxidation) in this section have led to calcite dissolution.

3.4 Water chemistry and redox environment

A summary of in-situ parameters and water chemistry for the study period is given in Table 2 for RW, the average concentrations in the HZ and in GW at 1 and 16 m from the river bank (GW1 and GW3, respectively), and GW4 (for information on SoilW, see Appendix A Table S2). The pH ranged from 6.8 to about 8.3 in all samples. The highest values were observed in the RW in March 2014. This decrease in acidity could indicate absorption of CO_2 by photosynthesizing algae. Concurrent oxygen levels higher than saturation levels support this. At the same time in the previous year, pH also peaked and then decreased (especially in the HZ and the GW) until the end of the rainfall season/the harvest of the maize. EC values were generally high in both RW and GW, ranging 1.2-1.5 mS/cm. A slight decrease of the EC was observed during the rainy summer months, probably caused by the dilution effect of the precipitation.

With regards to the ions Ca^{2+}, Na^{+}, Mg^{2+}, Cl^{-}, and HCO_3^{-}, differences over time and between samples were relatively small. Higher spatial differences were observed for sulfate, which was lower in the HZ than in other samples,

and potassium, which was very high (ranging 0.46-0.58 mmol/L) in the RW, and then notably decreased along the flow path into the field. Even though surface runoff from fertilizer applications can be one of the causes for high potassium loads in rivers, other sources must be responsible for the homogenous distribution across the entire year.

Table 2. Water chemistry of river water, hyporheic zone, and groundwater (groundwater sampled 1, 6 and 42 m from the river bank, respectively) from March 2013 to March 2014

Date	T	DO	pH	HCO_3^-	EC*	Na^+	K^+	NH_4^+	Ca^{2+}	Mg^{2+}	Cl^-	NO_3^-	SO_4^{2-}	Al^{3+}	Fe^{2+}	Mn^{2+}
	°C	mg/L		meq/L	mS/cm	mmol/L								µmol/L		
12 Mar, 2013																
RW	11.3	7.3	8.0	6.6	1.4	5.07	0.48	0.81	2.01	1.51	4.16	0.24	1.32	1.34	1.13	1.28
HZ_{avg}	10.4	0.9	7.7	6.5	1.3	4.60	0.37	n.d.	2.27	1.66	4.44	0.05	0.91	41.62	12.81	9.61
$GW1_{avg}$	11.3	1.3	7.5	7.2	1.4	5.35	0.29	0.57	2.39	1.51	4.24	0.07	1.35	0.42	0.38	1.81
$GW3_{avg}$	7.4	0.8	7.4	6.5	1.3	5.00	0.03	n.d.	2.69	1.60	4.47	0.17	1.29	n.d.	0.19	0.42
GW4	5.4	0.9	7.6	6.7	1.4	5.20	0.05	n.d.	2.65	1.76	4.47	0.27	1.38	n.d.	0.12	0.07
13 Apr, 2013																
RW	18.1	6.8	7.9	8.6	1.4	5.00	0.48	0.84	2.23	1.56	3.60	0.37	1.14	n.d.	0.25	n.d.
HZ_{avg}	14.1	1.6	7.6	9.0	1.4	5.10	0.41	1.03	2.35	1.62	4.06	0.02	0.61	101.35	40.46	11.18
$GW1_{avg}$	15.2	2.8	7.6	7.6	1.4	5.30	0.40	0.91	2.29	1.44	3.66	0.14	0.94	2.78	2.53	1.32
$GW3_{avg}$	10.5	0.4	7.4	7.5	1.4	5.35	0.02	0.02	2.83	1.61	3.91	0.04	1.02	0.78	0.64	0.48
GW4	10.4	0.6	7.5	7.2	1.4	5.47	0.04	0.04	2.67	1.83	3.95	0.43	1.12	n.d.	0.52	n.d.
29 May, 2013																
RW	24.2	3.6	7.8	7.3	1.4	4.97	0.53	1.10	2.09	1.55	4.05	0.13	1.09	6.04	2.92	1.71
HZ_{avg}	22.2	3.4	7.5	7.8	1.4	4.60	0.42	1.01	1.89	1.32	4.11	0.01	0.50	21.86	15.28	10.90
$GW1_{avg}$	24.1	3.3	7.3	8.1	1.4	4.89	0.53	0.86	2.30	1.41	3.81	0.01	0.69	n.d.	5.51	6.76
$GW3_{avg}$	16.5	0.4	7.2	7.7	1.4	5.50	0.03	0.05	2.70	1.54	3.99	0.01	0.85	2.14	1.63	0.64
GW4	14.6	3.6	7.4	6.8	1.4	5.49	0.03	0.03	2.69	1.77	4.09	0.49	1.30	n.d.	1.07	0.09
22 Jul, 2013																
RW	28.5	8.0	7.9	7.2	1.3	4.43	0.51	1.21	1.95	1.46	3.21	0.21	0.99	0.02	0.56	0.49
HZ_{avg}	26.4	0.4	7.1	8.7	1.2	4.04	0.43	1.33	1.92	1.30	2.72	0.01	0.27	n.d.	13.74	12.27
$GW1_{avg}$	27.8	0.3	7.2	6.5	1.0	3.41	0.46	0.92	1.77	1.13	2.34	0.05	0.79	n.d.	2.84	4.52
$GW3_{avg}$	22.1	0.3	7.0	7.1	1.2	4.80	0.02	n.d.	2.30	1.29	2.45	0.44	0.85	n.d.	1.17	0.70
GW4	22.4	0.3	7.0	6.9	1.2	4.79	0.05	0.04	2.43	1.55	2.74	0.94	1.03	n.d.	1.06	0.27
17 Sep, 2013																
RW	23.5	4.5	7.7	6.9	1.2	4.37	0.48	1.23	1.97	1.45	3.57	0.04	1.10	3.02	1.82	0.62
HZ_{avg}	24.2	3.4	7.0	8.9	1.3	4.60	0.48	1.35	2.25	1.43	2.74	n.d.	0.65	n.d.	21.38	12.93
$GW1_{avg}$	24.1	3.2	7.2	8.0	1.3	4.95	0.44	0.80	2.39	1.46	3.24	n.d.	1.21	n.d.	2.85	10.58
$GW3_{avg}$	21.4	3.3	7.0	7.1	1.2	4.90	0.05	0.01	2.64	1.40	3.58	n.d.	1.02	n.d.	1.98	2.20
GW4	23.4	4.3	7.0	8.0	1.2	4.75	0.08	n.d.	2.59	1.54	3.43	0.01	1.10	n.d.	2.20	1.79
14 Nov, 2013																
RW	9.9	4.0	7.8	7.9	1.5	5.35	0.53	1.68	2.39	1.66	3.20	0.46	1.62	1.66	1.86	1.69
HZ_{avg}	14.0	0.5	7.3	9.0	1.3	4.20	0.40	1.41	2.21	1.42	2.74	0.03	0.63	35.23	47.49	15.87
$GW1_{avg}$	15.8	0.5	7.3	7.5	1.3	4.49	0.36	0.79	2.53	1.54	3.07	0.02	1.38	n.d.	1.85	13.73
$GW3_{avg}$	16.8	0.8	7.2	7.8	1.2	4.50	0.06	n.d.	2.70	1.41	2.83	0.01	1.17	3.23	2.87	3.95
GW4	15.6	0.4	7.2	8.3	1.3	4.62	0.07	0.03	2.78	1.76	2.66	0.01	1.22	n.d.	6.64	6.82
05 Jan, 2014																
RW	4.1	5.8	7.8	7.3	1.4	5.07	0.45	1.40	2.19	1.74	4.48	0.34	1.18	0.84	1.84	1.45
HZ_{avg}	-	-	-	-	-	-	-	-	-	-	-	-	-	-	-	-
$GW1_{avg}$	8.5	1.9	7.4	7.6	1.3	4.74	0.33	0.70	2.66	1.70	4.29	0.02	1.26	n.d.	1.81	13.58
$GW3_{avg}$	9.3	0.3	7.2	7.3	1.3	4.97	0.04	n.d.	2.93	1.66	4.36	0.02	1.17	n.d.	0.34	2.01
GW4	9.2	2.8	7.2	8.2	1.3	5.03	0.03	0.01	3.09	2.09	4.26	n.d.	1.26	n.d.	3.32	3.24
25 Mar, 2014																
RW	14.7	18.0	8.2	7.6	1.4	5.17	0.46	1.14	2.21	1.69	3.71	0.25	1.27	0.36	0.64	0.15
HZ_{avg}	-	-	-	-	-	-	-	-	-	-	-	-	-	-	-	-
$GW1_{avg}$	9.2	1.0	7.4	7.0	1.3	4.30	0.31	0.70	2.52	1.54	3.71	n.d.	1.17	n.d.	4.74	14.88
$GW3_{avg}$	9.8	1.0	7.2	7.8	1.2	4.49	0.05	n.d.	2.65	1.41	3.63	n.d.	1.13	n.d.	4.77	3.56
GW4	10.2	1.1	7.2	7.9	1.3	4.76	0.03	0.01	2.94	1.98	3.72	n.d.	1.23	n.d.	5.01	5.02

* = Compensated for 25°C, RW = River water, HZ_{avg} = Average of samples from the hyporheic zone, $GW1_{avg}$ = Average of samples at 1 m distance from the river, $GW3_{avg}$ = Average samples at 11 m distance from the river, GW4= Sample at 41 m distance from the river.

Potassium concentrations in domestic sewage in different countries are reported to be 10-30 mg/L (Arienzo et al., 2009). As this is in the same range as the detected concentrations (which are equivalent to 19.4 mg/L on average), discharge of wastewater into Fu River is the most likely reason for the elevated potassium in the river, which was then removed from solution in the GW. Overall, no dominant cation type could be determined, but bicarbonate is clearly the dominating anion in samples from all sampling points (see Figure 5). In all waters, calcium, and sodium + potassium dominated slightly over magnesium. Chloride concentrations are relatively high for continental waters, indicating sodium-calcium-bicarbonate-chloride water. The similarity between RW and the GW chemistry demonstrates the high degree of connection between the two environments.

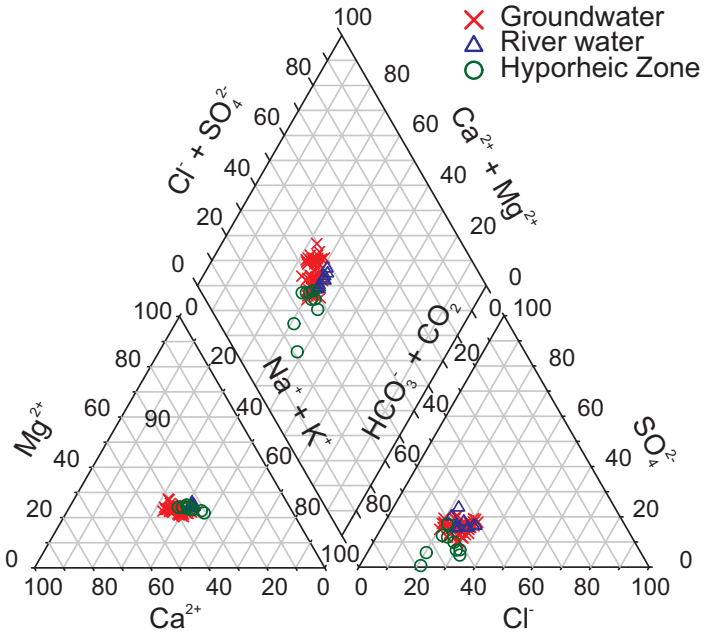

Figure 5. Piper plot showing the similarity in water types of groundwater, surface water and of water from the hyporheic zone.

Regarding different redox environments, it is notable that the major ion composition of samples from the HZ showed lower levels of sulfate than in other locations. As sulfate can be converted to hydrogen sulfide in strongly reducing environments, this indicates that the HZ offers a distinctly different environment in which sulfate reduction occurs. This assumption is supported by low oxygen values in the HZ, and by the minor ion analysis, which shows elevated levels of dissolved manganese and iron ions ranging up to 16.6 and 60.6 µmol/L, respectively (see Figure 6). Even though oxygen levels were close to zero at some of the GW samples (2), only very little dissolved

manganese and iron was detected (or none at all), and sulfate values were similar to the ones in the RW. Therefore, it seems like no manganese, iron, or sulfate reduction takes place in the GW at the sampled depth, though nitrate reduction may be possible. Even though the water flow was assumed to be RW → HZ → GW1 →…→ GW4 based on the results summarized in section 2.2, the elevated concentrations of sulfide from the HZ do not propagate into the GW sampling points. This might mean that either a re-oxidation process is going on, or that the water received at the GW wells comes from higher points of the river bank with less reducing conditions (for technical reasons, the screens for GW sampling had to be installed 50 cm higher than those of the HZ).

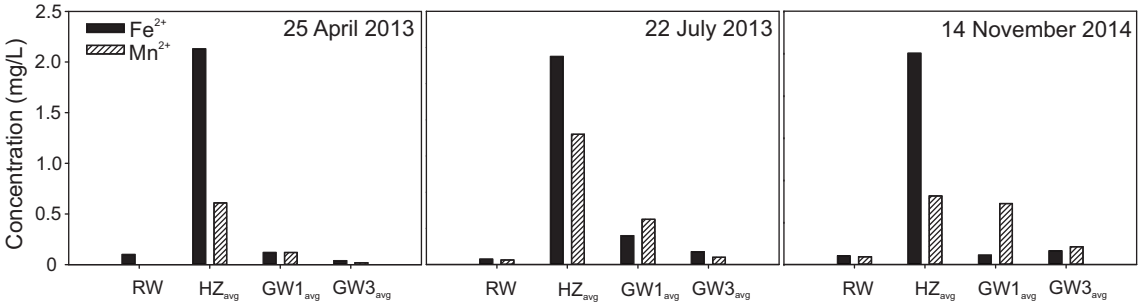

Figure 6. Dissolved iron and dissolved manganese concentrations at different times of the year in river water (RW), the hyporheic zone (HZ_{avg}) in groundwater (GW) samples 1 m ($GW1_{avg}$) and 6 m ($GW3_{avg}$) from the river bank (samples filtered in situ through a 0.45 µm cellulose-ester membrane and acidified immediately to pH=2 using concentrated HNO_3). Values for HZ and GW1+3 are given as average values from both sampling lines.

3.5 Speciation with PHREEQC

Mean values and ranges of saturation indices (SI) for different minerals and P_{CO_2} were calculated with PHREEQC (see Fig. 7 and Fig.8 for temporal representation of selected results, and Appendix A Table S3 for more detailed information). SI other than 0 indicate undersaturation (SI<0) or oversaturation (SI>0) of a solution with respect to the given mineral, so that the potential for mineral dissolution or precipitation (respectively) can be concluded. SI for calcite and aragonite (both $CaCO_3$) ranged between -0.13 to 1.20 and -0.27 to 1.05, respectively. The higher values generally corresponded to RW and SoilW samples, while the lower values mostly referred to GW and the HZ. Dolomite ($CaMg(CO_3)_2$) saturation had a higher variation, ranging from -0.40 to 2.30, but showed similar distribution with the highest saturation values in RW and SoilW. All three minerals had slightly

lower SI during the summer months. The calculated P_{CO_2} ranged from 0.29-6.58%, with generally higher values in GW and HZ than in SoilW and RW. P_{CO_2} in GW samples especially increased during the warmer months of the year, when soil respiration is known to increase (Boone et al., 1998). Generally, the PHREEQC calculation indicates that precipitation of carbonate is slightly more likely to take place, though dissolution processes may also occur, especially in the soil system during the summer months.

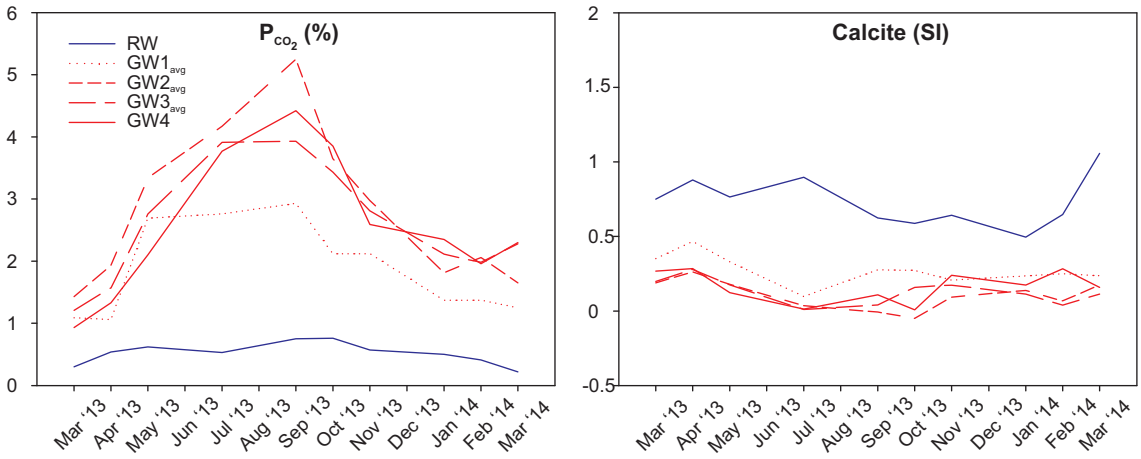

Figure 7. P_{CO_2} and saturation indices (SI) for calcite in river water (RW) and groundwater (GW) samples GW1-GW4 over time. Calculation was done with PHREEQC.

3.6 Nitrogen species

3.6.1 Occurrence

In this study, nitrate concentrations in SoilW reached up to 9.5 mmol/L (134.8 mg/L NO_3-N), and suggest that nitrate leaching into the shallow aquifer might occur at this site (RW concentrations were much lower, and therefore only the vertical infiltration from the field surface is discussed in terms of pollution source for nitrate). The average amount of nitrate detected at SoilW1.2 was 0.7 mmol/L (10.3 mg NO_3-N), which is above allowed levels for drinking water (only data from the first part of the study was considered, when regular agricultural activities took place). However, only relatively low amounts of nitrate averaging around 0.1 mmol/L (1.3 mg/L NO_3-N) were detected in GW (see Figure 8). Other recent studies in the NCP detected average NO_3-N concentrations that clearly exceeded the national standard for GW of 10 mg/L (Huang et al., 2011), so the results at our study site are surprising, and indicate that effective nitrate removal processes must take place.

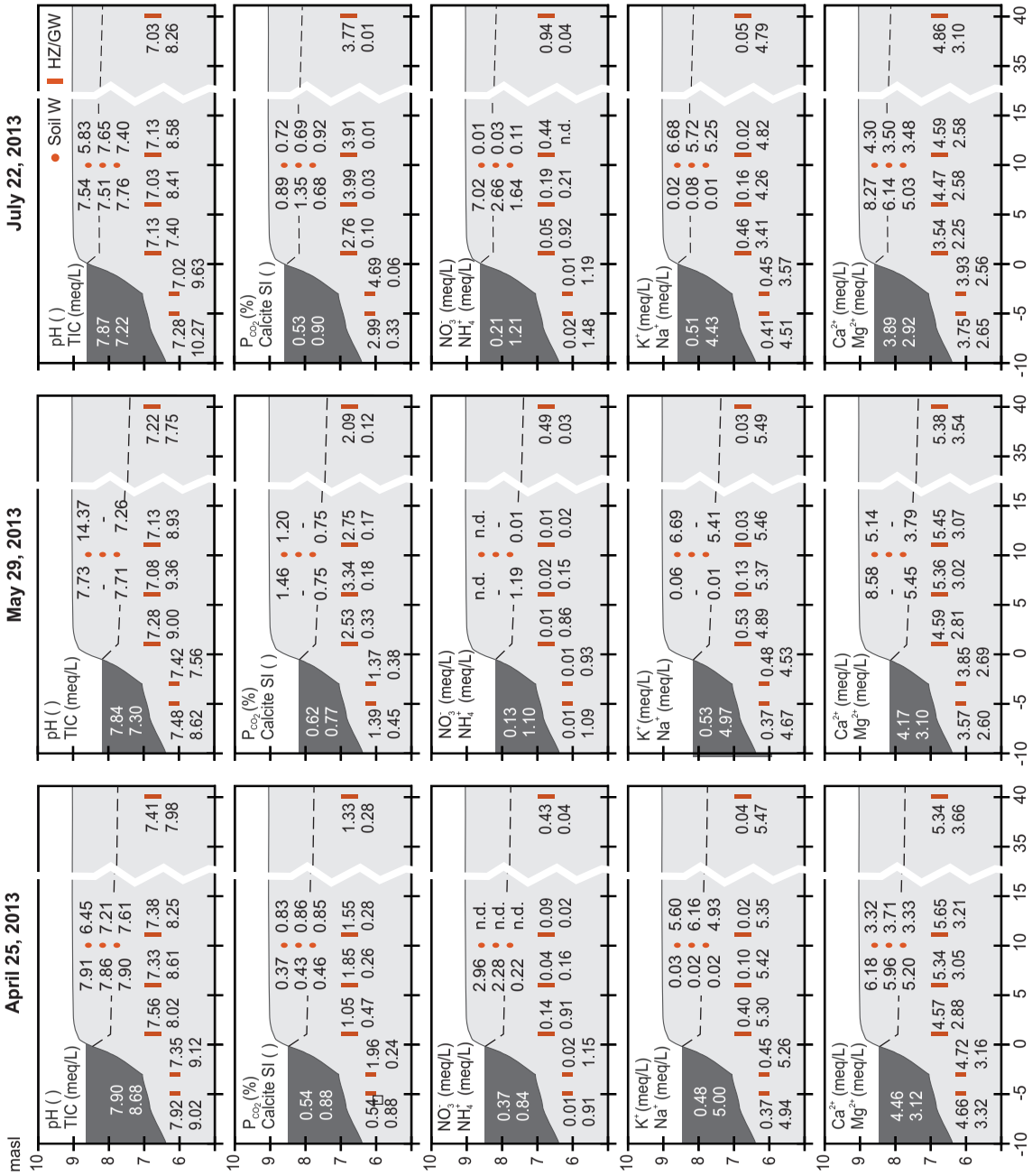

Figure 8. Cross-section of the sampling site showing average values from both sampling lines for pH, selected results from the speciation calculated with PHREEQC (TIC, P_{CO_2}, and calcite saturation), and measured concentrations of nutrients (NO_3^-, NH_4^+, K^+) and other ions (Na^+, Ca^{2+}, and Mg^{2+}), in April, May and July 2013.

Ammonium was found in large concentrations of up to 1.7 mmol/L (29.8 mg/L NH_4-N) in RW, with peak values occurring from July-October. This compares well to reported measurements of 1.1 mmol/L at Fu River in 1992 (Muqi et al., 1998). Similar values were found in the HZ, while concentrations in the wells below the field area (GW2-4) averaged at 0.1 mmol/L (1.1 mg/L NH_4-N). As it is known that Fu River receives a lot of wastewater discharge along its flow path through Baoding City, the most likely explanation for the concurrent occurrence of ammonium and nitrate (and smaller amounts of nitrite) is that the input of ammonium is so high that the river system cannot convert the entire amount to nitrate, as it would occur in more natural systems. The clear decline in ammonium concentrations in the aquifer indicates efficient ammonium removal processes in the system.

3.6.2 Suggested removal mechanisms for nitrogen species

Nitrate is a main agricultural pollutant, which has a high potential to leach into GW, as it neither binds to clay minerals nor forms insoluble compounds with other elements in the subsurface. Nitrate that enters the soil system can be assimilated (e.g., uptake by plants), denitrified, reduced to ammonium by dissimilatory nitrate reduction (DNRA), or used in the anammox process to form dinitrogen (which will be further discussed in the next paragraph). In places, where OM is abundant, nitrate degradation via OM is likely to occur:

$$5CH_2O + 4\,NO_3^- \rightarrow 2N_2 + 4HCO_3^- + H_2CO_3 + 2H_2O \qquad \text{(Equation 1)}$$

Other electron donors aside from OM such as pyrite or ferrous iron, could also be used, but are often not as abundant, and the energy yield of the nitrate reduction is lower, so that degradation via OM is the favoured process, though kinetics of pyrite oxidation may be faster (Appelo and Postma, 2005).

Ammonium can either be bound to the soil by CE, or degraded by nitrification processes (in aerobic environments) or anammox (Buss et al., 2004). Among these options, CE is the simplest process that reduces the dissolved ammonium concentration. The positively charged ammonium ions are adsorbed to clay particles in the soil under exchange with previously bound ions, such as K^+, Na^+, Mg^{2+}, or Ca^{2+}. Under aerobic conditions, ammonium can be nitrified, and each mole of ammonium produces two moles of hydrogen ions (H^+):

$$NH_4^+ + 2O_2 \rightarrow NO_3^- + H_2O + 2\,H^+ \qquad \text{(Equation 2)}$$

If these two protons cause calcite dissolution, free bicarbonate and Ca^{2+} will form along with the nitrification:

$$2CaCO_3 + 2\,H^+ \rightarrow 2\,Ca^{2+} + 2\,HCO_3^- \qquad \text{(Equation 3)}$$

The anammox process, on the other hand, takes place anaerobically. Within the process, ammonium reacts with nitrite and forms molecular nitrogen:

$$NH_4^+ + NO_2^- \rightarrow N_2 + 2H_2O \qquad \text{(Equation 4)}$$

It has been shown by labelling experiments that partial degradation of nitrate is a major source of nitrite in this reaction (Thamdrup and Dalsgaard, 2002), and a recent study on Chinese paddy soil identified the anammox process to contribute 4-37% to the dinitrogen production to different layers in the soil (Zhu et al., 2011). Furthermore, a study using denaturing gradient gel electrophoresis (DGGE) on an upstream sampling site of Fu River has shown that denitrifying and anaerobic ammonium oxidizing bacteria is abundant throughout the year, with Shannon-Wiener indices of up to 1.53 and 2.07, respectively (Qi et al., 2012) .

In this study, measured DO suggested slightly anoxic conditions in the GW system throughout most of the year. In the HZ, increased concentrations of dissolved manganese and iron, along with a decrease in sulfate, indicated a strongly reducing environment. Therefore, anaerobic reduction processes, such as denitrification, DNRA, and anammox are likely removal process. The high clay content of the soil also produces good conditions for CE of ammonium. As Figure 9 shows, there seems to be an inverse relationship between dissolved ammonium and calcium ($r=0.74$, $P<0.0001$), indicating adsorption of ammonium to the exchanger (the soil surface) under the release of calcium. However, two moles of ammonium would be necessary to release one mole of calcium, which would not produce a 1:1 relationship. The reverse holds true for nitrification with subsequent calcite dissolution, in which case one mole of oxidized ammonium could cause two moles of calcium to be released (Equation 2 and 3). The apparent 1:1 relationship indicates that both processes may play a role. Even though only small amounts of DO were measured, nitrification of the ammonium by oxygen might be possible if more oxygen is temporarily present. However, the denitrification rate and the uptake of ammonium from CE would need to be very high in order to compensate for the large decrease in dissolved GW concentration of both nitrogen species. Additional partial degradation of nitrate and its use in anammox could be an explanation of this.

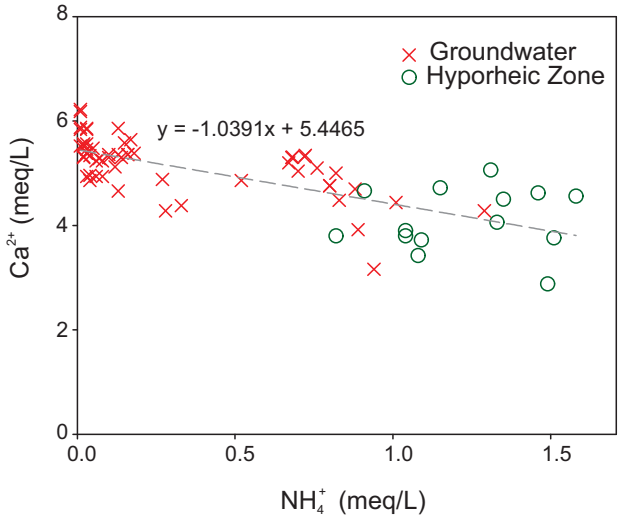

Figure 9. Scatter plot of ammonium versus calcium ions, showing the inverse relationship of the two ions in the hyporheic and groundwater zone (samples with NH_4^+ = 0 meq/L were excluded from this graph).

3.7 PHREEQC 1-D simulation of potential removal processes

The processes described in the previous section can be combined leading to a complex system, so in addition to the speciation calculation, a simple 1-D horizontal transport model in PHREEQC with different set-ups (described in section 1.5) was used to simulate hydrogeochemical effects of the RW flowing into the aquifer. Because farming activities did not take place after October 2012 due to danger of flooding (section 2.2.), we only considered the period from March-September 2012 in our model. A comparison of simulated results versus measured values for pH, alkalinity, and selected ions (K^+, NH_4^+, NO_3^-, and SO_4^{2-}) can be seen in Figure 10 for the different models. The first column shows selected results (the model step from April-May 2013) for the effects of RW infiltration when only CE is considered (CE Model). Especially the rapid decline of the high potassium concentrations, and the absorption of ammonium ions onto the soil are well represented in this model. Decreasing amounts of calcium on the exchanger sites are observed, and indicate the exchange of ammonium and potassium ions with the calcium ions. Calibration of the model indicated that the current flow direction could be a relatively recent feature of the system because longer equilibration phases (e.g. 3 years) resulted in dissolved potassium concentrations higher than the observed ones.

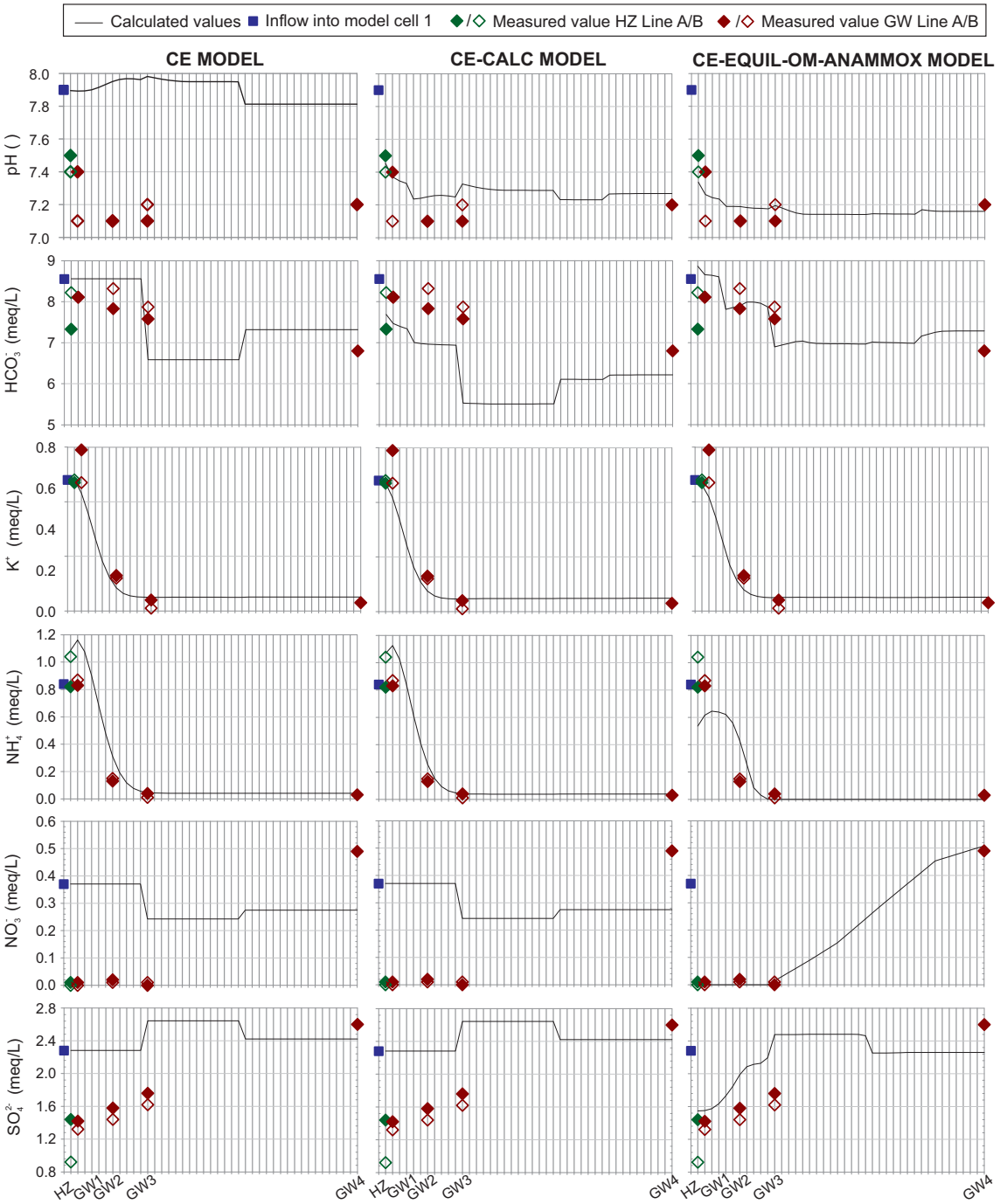

Figure 10. Results of the three different model setups in PHREEQC for selected parameters, and measured concentrations in the hyporheic zone (HZ) and at groundwater (GW) sampling points GW1-GW4. Model results refer to the simulated step from April to May 2013.

This is due to the fact that the exchanger sites in the soil gradually cease to absorb more potassium ions. Simulated values for alkalinity followed roughly the observed pattern. However, variations for nitrate and sulfate could not be reflected, and pH values were generally too high, which clearly showed that other processes needed to be included. For the second setup (CE-Calc Model), represented in the central column on Figure 10, calcite equilibrium (based on calculated for SI's for different sections) was added. In this model, changes in pH were very well reflected, and uptake of ammonium and potassium remained the same as in the previous setup. However, calculated alkalinity was noticeably lower (up to 2 mmol/L) than the measured values, and processes for nitrate degradation still needed to be included. The third column on Figure 10 shows the results of the CE-Equil-OM-Anammox Model, which included degradation of OM in the HZ (and to a lesser degree in the GW), and anammox in addition to CE, calcite, and iron(II) sulfide equilibrium. Iron hydroxide was added in the HZ to simulate observed iron (III) reduction, and in the GW, low levels of oxygen and varying vertical input of nitric acid derived from oxidation of urea (applied in March 2013) and compound fertilizer (applied in June 2013) were added, to reflect the field conditions more accurately. The amount of OM was varied according to assumed root production during the different stages of the wheat cultivation. With these changes, the model was able to reproduce the low nitrate levels in the first meters of the field, as well as the increases in nitrate towards GW4 that were observed in May 2013. Compared to other months, where more nitrate was removed from the system, the model suggests that the assumingly lower amount of OM in the soil in the early growing stages of the wheat is a limiting factor for the nitrate removal capacity of the soil-GW-system, as it means that less electron donors are present. Furthermore, the concurrent build-up of nitrate after depletion of dissolved ammonium from the GW, could suggest that anammox plays a significant role in the nitrate removal process at the studied site.

To test the hypothesis that ammonium levels might have a strong influence on nitrate removal, and to see what would happen if more pristine water with lower ammonium pollution would enter the GW, the the model parameters were changed to an ammonium load of the RW of only 0.02 mmol/L (Clean River Model). Results from for the "Present-Model" (the previous CE-Equil-OM-Anammox Model without input changes), the Clean-River Model, and measured values for model cell 42, (representing GW sampling point GW4), are shown in Figure 11. During all of the simulated period, nitrate levels

increased noticeably when ammonium input was reduced. The difference between nitrate values simulated for observed ammonium input and low ammonium input ranged between 0.17-0.35 mmol/L, and on average, this corresponded to 1.7 times higher concentrations of nitrate in the GW. This shows that anammox, along with denitrification processes, plays an important role in the removal of nitrate.

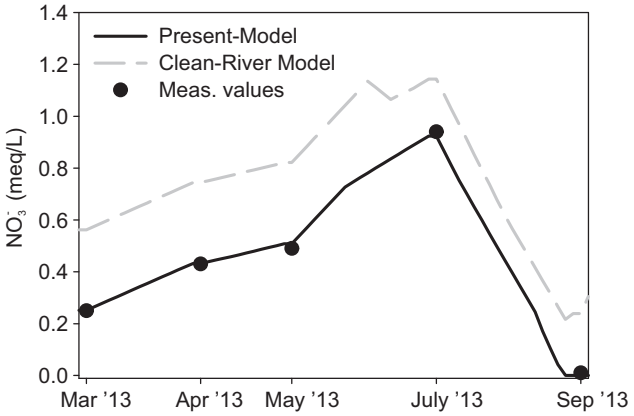

Figure 11. Simulation results for model cell 42 for the CE-Equil-OM-Anammox Model using measured ammonium concentrations as input (Present Model), and with ammonium levels reduced to 0.02 mmol/L (Clean River Model) in the input solution.

Overall, our PHREEQC simulations produced a model that could reflect the observed field conditions, and the removal of nitrogen and potassium reasonable well. Smaller deviations from the measured values are still present, but this was to be expected since relatively long periods (up to 55 days) between the sampling periods had to be modelled with a constant input concentration of the parameters, while the chemical composition in the field naturally changed gradually. Due to this relatively low temporal resolution, the main focus of our model was rather to identify pathways and correlations between parameters rather than the exact quantification of each process. The dominant removal mechanisms included CE, denitrification via OM, and anammox. To further test if the hypothesized processes play part in the removal pathways in the field, isotope pairing using N-15 isotopes as applied by Uldahl et al. (2013) could be used.

3.8 Conceptual model, future trends and monitoring

A conceptual model is shown in Figure 12 to summarize the inputs and outputs of nitrogen species and the simulated removal mechanisms down to 2 m below the GW table. Nitrogen input includes estimated values from

fertilizer application, inflow from the river, and wet atmospheric deposition. Fertilizer-N input has been calculated based on interviews with the farmer on application rates, and product information of the fertilizer. Different literature sources were used to estimate the average N-uptake by harvested crop and the amount of nitrogen in remaining stubbles and stems (Liu et al., 2003; Vitousek et al., 2009; Zhao et al., 2006). Wet deposition was calculated based on literature values for nitrogen concentrations in precipitation in the BYD catchment (Zhang et al., 2008), actual amount of rainfall during the study period, and the amount of nitrogen input from irrigation with the RW. Volatilization was estimated based on a study on ammonia volatilization from urea application (Yang et al., 2011), and under consideration that not only urea, but also other fertilizers were applied at our site (which are less prone to volatilization). Inflow of nitrogen from the river is based on the average N-values from the entire sampling period in RW, which were then multiplied with the depth of the river, an assumed average GW flow velocity of 100 m/year, a literature value for porosity of silty clay loam (0.44), and a width of the field of 100 m. This value represents the amount of nitrogen that flows in under a one hectare area. Horizontal outflow was calculated in a similar way, using the average measured N-concentrations at GW4 and a depth of GW equal to 2 m. Vertical outflow assumes an infiltration rate of 175 mm/year, derived from literature studies on soil water drainage within comparable regions of the NCP (Cao et al., 2014; Zhang et al., 2004), and from our own observation that drainage seemed to be relatively high.

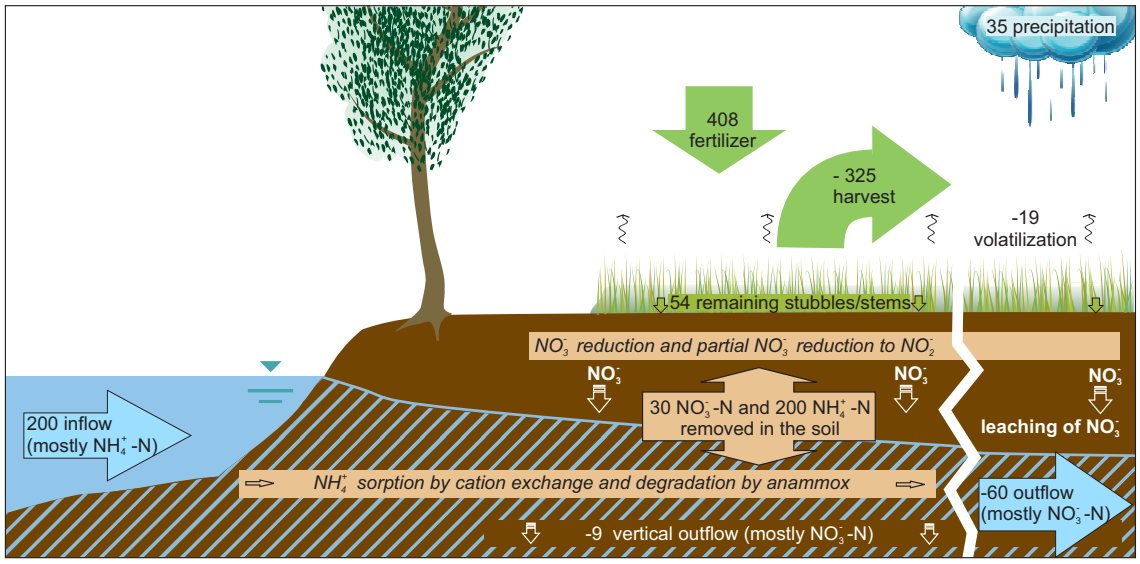

Figure 12. Conceptual model summarizing the inputs and outputs in kg/ha/a of nitrogen species, vertical leachate of nitrate, and suggested removal mechanisms.

As can be seen, nitrogen inputs compared to harvest outputs are in excess by roughly 320 kg/ha/a. Yet, both ammonium and nitrate have only been detected in low concentrations in GW samples, which indicates efficient removal processes. The dominant removal mechanisms identified in this study are full reduction by OM as well as partial reduction to nitrite and subsequent consumption in the anammox process for nitrate, and CE and anammox for ammonium. The entire instreaming amount of ammonium from the river seems to be depleted by CE and anammox. About 99 kg NO_3^--N/ha/year enter the soil system via vertical leaching, of which 30% are degraded, 9% leach further downwards, and 61% propagate further into the field with the horizontal flow. The measured average concentration of nitrate at GW4 was 3.5 mg NO_3^--N/L, which is still an acceptable value. However, as our results from the PHREEQC model indicate (section 2.7.) that concentrations of nitrate may further increase along the GW flow deeper into the field. Furthermore, averaging the observed nitrate concentrations in GW samples may not well reflect periods in which higher concentrations are leached, and our relatively large time intervals between samplings may not have caught the actual peak values. Intermittently higher nitrate concentrations in the GW can therefore not be excluded.

3.9 Future trends, implications, and representativeness for the BYD region and NCP

Despite the apparent current capacity of the soil system at the studied site to cope with most of the incoming pollutants, we think that the intense agriculture combined with large amounts of nitrogen fertilizer input, may pose a threat to the quality of the shallow aquifer. This would especially be the case when the aquifer is aerobic for longer timeframes (which enhances nitrification and hinders anammox and denitrification), or when the availability of ammonium for anammox is decreased (e.g., due to upstream wastewater treatment or a change in flow direction between the aquifer and the surface water). Ammonium is an indicator for poor surface water quality, and more efficient wastewater treatment would be recommended, but our results (Figure 11) show that it is important to monitor the nitrate concentrations in the shallow aquifers while such measures are taken. Furthermore, even if instreaming nitrogen in the river would be reduced, fertilization would still be in excess and could probably be reduced to about 230 kg/ha/a of nitrogen, which is in accordance with other recommendation from studies in the NCP (Liu et al., 2003; Zhao et al., 2006).

Few studies on the interaction and nutrient exchange of surface water and GW in the BYD region have been published in the past. Moiwo et al. (2010) found that GW drawdowns around Baiyang Lake cause a leakage of lake water into the underlying aquifer system. Yuan et al. (2012) studied the impacts of percolation in the BYD region on GW via stable isotope techniques, and found that the shallow GW receives its main recharge from surface water such as Baiyang Lake itself, or other large water bodies, such as the Tang sewage reservoir (which impacts GW quality). These findings support that the same flow direction of surface water into the shallow aquifer—as observed in our own study—seems to be typical for the ambient BYD region. Additionally given the fact that the area is relatively homogenous in terms of geology, hydrogeology and agricultural production, we therefore presume that our results on nutrient exchange and degradation could be representative for much of this region. Regarding the NCP, most of the alluvial plain (Heilonggang) is characterized by silty to clayey soil, nearly level terrain, and similar climate to the study region. Even though infiltration of precipitation is the main recharge mechanism for most of the shallow GW in the NCP, leakage of surface water has also been observed (Li et al., 2014; Liu et al., Yuan et al., 2011; Zhang et al. 2014). Furthermore, surface water pollution by increased ammonium levels is common in many of the rivers (MEP, 2014). Several findings of ammonium oxidizing bacteria in East China (including the NCP) as summarized by Ali et al. (2013) imply that similar results to the ones at our field study might be possible also in specific parts of the NCP, where contaminated surface water recharges the GW with good hydraulic connection.

4 Conclusion

Pollutant exchange between RW and GW, and nutrient removal pathways at a wheat-maize double cropping area in the NCP were investigated based on RW, GW, and SoilW samples from a one-year field study. This paper shows that the GW, as well as the soil system at the studied field site, is currently highly influenced by the instreaming RW. The river system is not able to nitrify its ammonium load of up to 29.8 mg/L NH_4-N despite sufficient oxygen availability, and it is therefore transported into the shallow aquifer system. Here, almost all of the ammonium is currently bound to the soil by CE, converted to N_2 by anammox, or potentially oxidized in intermittent aerobic conditions in the shallow aquifer. Ammonium concentrations in the

GW wells below the field area did not exceed more than 2.2 mg/L NH_4-N. Despite high fertilizer inputs, nitrate values in the GW and RW averaged around 2 mg/L NO_3-N, which is well below the national standard for GW (10 mg/L NO_3-N). However, substantial amounts of nitrate seem to leach into the aquifer, and nitrate concentrations generally increase along the flow path. Denitrification and partial denitrification with subsequent nitrite degradation by anammox were identified as important removal processes for nitrate during the timeframe of the study. It is recommended that nitrate is closely monitored in the system if the river is cleaned up, and that generally, nitrate inputs are reduced, and should be applied based on measured soil requirements, rather than on traditional practice.

Acknowledgements

The authors would like to thank the Sino-Danish Centre for Education and Research, and the Technical University of Denmark for funding this project. Special thanks go to Wenjia Wang, Xiangmin Sun, Bing Zhang, Zhenyu Sun, Yilei Yu, Baogang Jiang, and Lihu Yang from the Institute of Geographic Sciences and Natural Resources Research, Beijing, for their generous assistance and support of the conducted field work; Farmer Ma in Dongxiangyang Village for his agreement to use his land and for his help, Ruiqiang Rui for sharing his expertise and data on the case study area, and Fritz Hamme for language revision.

References

Ali, M., Chai, L., Tang, C., Zheng, P., Min, X., Yang, Z., Xiong, L., Song, Y., 2013. The increasing interest of ANAMMOX research in China: bacteria, process development, and application. Biomed. Res. Int. 2013, 1-21.

Appelo, C. A. J.; Postma, Dieke (2005): Geochemistry, groundwater and pollution. (2nd ed.), Balkema, New York, USA.

Arienzo, M., Christen, E.W., Quayle, W., Kumar, A., 2009. A review of the fate of potassium in the soil-plant system after land application of wastewaters. J. Hazard. Mater. 164 (2-3), 415–422.

Boone, R.D., Nadelhoffer, K.J., Canary, J.D., Kaye, J.P., 1998. Roots exert a strong influence on the temperature sensitivity of soil respiration. Nature. 396, 570–572.

Buss, S.R., Herbert, A.W., Morgan, P., Thornton, S.F., Smith, J. W. N., 2004. A review of ammonium attenuation in soil and groundwater. Q. J. Eng. Geol. Hydroge. 37 (4), 347–359.

Cao, G., Han, D., Song, X., 2014. Evaluating actual evapotranspiration and impacts of groundwater storage change in the North China Plain. Hydrol. Process. 28 (4), 1797–1808.

Chen, J., Tang Changyuan, Sakura, Y., Yu, J., Fukushima, Y., 2005. Nitrate pollution from agriculture in different hydrogeological zones of the regional groundwater flow system in the North China Plain. Hydrogeol. J. 13 (3), 481–492.

Costa, J., Massone, H., Martínez, D., Suero, E., Vidal, C., Bedmar, F., 2002. Nitrate contamination of a rural aquifer and accumulation in the unsaturated zone. Agr. Water Manage. 57 (1), 33–47.

Devlin, J.F., 2015. HydrogeoSieveXL: an Excel-based tool to estimate hydraulic conductivity from grain-size analysis. Hydrogeol. J. 23 (4), 837–844.

Dikgwatlhe, S. B.; Kong, F. L.; Chen, Z. D.; Lal, R.; Zhang, H. L.; Chen, F.; Goss, Michael (2014): Tillage and residue management effects on temporal changes in soil organic carbon and fractions of a silty loam soil in the North China Plain. Soil Use Manage. 30 (4), pp. 496–506.

Huang, J., Xu, J., Liu, X., Liu, J., Wang, L., 2011. Spatial distribution pattern analysis of groundwater nitrate nitrogen pollution in Shandong intensive farming regions of China using neural network method. Math. Comput. Model. 54 (3-4), 995–1004.

Ju, X.T., Kou, C.L., Zhang, F.S., Christie, P., 2006. Nitrogen balance and groundwater nitrate contamination: comparison among three intensive cropping systems on the North China Plain. Environ. Pollut. 143 (1), 117–125.

Lettens, S., Vos, B. de, Quataert, P., van Wesemael, B., Muys, B., van Orshoven, J., 2007. Variable carbon recovery of Walkley-Black analysis and implications for national soil organic carbon accounting. Eur. J. Soil Sci. 58 (6), 1244–1253.

Li, H., Liu, Z., Lei, Y., 2011. Resilience analysis for agricultural systems of North China Plain based on a dynamic system model. Sci. Agric. 68 (1), 8–17.

Li, J., Li, F., Liu, Q., Zhang, Y., 2014. Trace metal in surface water and groundwater and its transfer in a Yellow River alluvial fan: evidence from isotopes and hydrochemistry. Sci. Total Environ. 472, 979–988.

Li, Z.; Hu, K.; Li, B.; He, M.; Zhang, J. (2015): Evaluation of water and nitrogen use efficiencies in a double cropping system under different integrated management practices based on a model approach. Agr. Water Manage. 159, 19–34.

Liu, J., Zheng, C., Zheng, L., Lei, Y., 2008. Ground water sustainability: methodology and application to the North China Plain. Ground water. 46 (6), 897–909.

Liu, J., Cao, G., Zheng, C., 2011. Sustainability of Groundwater Resources in the North China Plain. Sustain. Groundw. Resour. 69–87.

Liu, X., Ju, X., Zhang, F., Pan, J., Christie, P., 2003. Nitrogen dynamics and budgets in a winter wheat–maize cropping system in the North China Plain. Field Crop. Res. 83 (2), 111–124.

Mao, X., Yang, Z., 2011. Functional assessment of interconnected aquatic ecosystems in the Baiyangdian Basin—An ecological-network-analysis based approach. Ecol. Model. 222 (23-24), 3811–3820.

MEP, 2014. 2013 Report on the State of the Environment of China. Available at: http://www.gzhjbh.gov.cn/images/dtyw/tt/gndttt/2014/6/5/7e4df35f-d266-429e-8269-6eba756c24f8.pdf. Date accessed: 20 August 2015. (in Chinese)

Moiwo, J.P., Yang, Y., Li, H., Han, S., Yang, Y., 2010. Impact of water resource exploitation on the hydrology and water storage in Baiyangdian Lake. Hydrol. Process. 24 (21), 3026–3039.

Muqi, X., Jiang, Z., Yuyao, H., Yurong, G., Shen, Z., Yijian, T., Chengqing, Y., Zijian, W., 1998. The Ecological Degradation and Restoration of Baiyangdian Lake, China. J.Freshwater Ecol. 13 (4), 433–446.

Nelson, G. C. (2010): Food security, farming, and climate change to 2050. Scenarios, results, policy options. Washington, D.C.: International Food Policy Research Institute (IFPRI research monograph).

Parkhurst, D.L., and Appelo, C.A.J., 2013, Description of input and examples for PHREEQC version 3--A computer program for speciation, batch- reaction, one-dimensional transport, and inverse geochemical calculations: U.S. Geological Survey Techniques and Methods, book 6, chap. A43, 497 p., Available at: http://pubs.usgs.gov/tm/06/a43. Date accessed: 20 August 2015.

Qi, Y., Wang, Z., Pei, Y., 2012. Evaluation of water quality and nitrogen removal bacteria community in Fuhe River. Procedia Environ. Sci. 13, 1809–1819.

Qiu, R., Li, Y., Yang, Z., Shi, J., 2009. Influence of water quality change in Fu River on Wetland Baiyangdian. Front. Earth Sci. China 3 (4), 397–401.

Rupert, M.G., 2008. Decadal-scale changes of nitrate in ground water of the United States, 1988-2004. J. Environ. Qual. 37 (5 Suppl), S240-8.

Sheldrick, W. F.; Syers, J. K.; Lingard, J. (2003): Soil nutrient audits for China to estimate nutrient balances and output/input relationships. Agr. Ecosyst. Environ. 94 (3), pp. 341–354.

Strebel, O., Duynisveld, W., Böttcher, J., 1989. Nitrate pollution of groundwater in western Europe. Agr. Ecosyst. Environ. 26 (3-4), 189–214.

Thamdrup, B., Dalsgaard, T., 2002. Production of N_2 through Anaerobic Ammonium Oxidation Coupled to Nitrate Reduction in Marine Sediments. Appl. Environ. Microb. 68 (3), 1312–1318.

Uldahl, A., Thamdrup, B., Jakobsen, R., 2013. Anammox in an ammonium-impacted groundwater aquifer. Mineral. Mag. 77 (5), 2375.

Vitousek, P.M., Naylor, R., Crews, T., David, M.B., Drinkwater, L.E., Holland, E., Johnes, P.J., Katzenberger, J., Martinelli, L.A., Matson, P.A., Nziguheba, G., Ojima, D., Palm, C.A., Robertson, G.P., Sanchez, P.A., Townsend, A.R., Zhang, F.S., 2009. Agriculture. Nutrient imbalances in agricultural development. Science. 324 (5934), 1519–1520.

Wang, W., Wang, D., Yin, C., Chen, H., Jiang, J., Zheng, J., 2001. A study on the ground water quality of the Baiyangdian wetland ecosystem. Acta Ecol. Sin. 21 (6), 919–925.

Yang Z. P., Turner D. A., Zhang J. J., Wang Y. L., Chen M. C., Zhang Q., Denmead O. T., Chen D., Freney J. R. (2011) Loss of nitrogen by ammonia volatilisation and denitrification after application of urea to maize in Shanxi Province, China. Soil Res. 49, 462–469.

Yuan, R., Song, X., Zhang, Y., Han, D., Wang, S., Tang, C., 2011. Using major ions and stable isotopes to characterize recharge regime of a fault-influenced aquifer in Beiyishui River Watershed, North China Plain. J. Hydrol. 405 (3-4), 512–521.

Yuan, R., Song, X., Wang, P., Zhang, Y., Wang, S., Tang, C., 2012. Impacts of percolation in Baiyangdian Lake on groundwater. Adv. Water Sci. (6), 751–756. (in Chinese)

Zhang, W.L., Tian, Z.X., Zhang, N., Li, X.Q., 1996. Nitrate pollution of groundwater in northern China. Agr. Ecosyst. Environ. 59 (3), 223–231.

Zhang, Y., Liu, X.J., Fangmeier, A., Goulding, K., Zhang, F.S., 2008. Nitrogen inputs and isotopes in precipitation in the North China Plain. Atmos. Environ. 42 (7), 1436–1448.

Zhang, Y., Kendy, E., Qiang, Y., Changming, L., Yanjun, S., Hongyong, S., 2004. Effect of soil water deficit on evapotranspiration, crop yield, and water use efficiency in the North China Plain. Agric. Water Manage. 64 (2), 107–122

Zhang, Y., Li, F., Zhang, Q., Li, J., Liu, Q., 2014. Tracing nitrate pollution sources and transformation in surface- and ground-waters using environmental isotopes. Sci. Total Environ. 490, 213–222.

Zhao, J., Guo, J., 2013. Possible Trajectories of Agricultural Cropping Systems in China from 2011 to 2050. AJCC 02 (03), 191–197.

Zhao, R., Chen, X.-, Zhang, F., Zhang, H., Schroder, J., Römheld, V., 2006. Fertilization and Nitrogen Balance in a Wheat–Maize Rotation System in North China. Agron. J. 98 (4), 938.

Zhu, G., Wang, S., Wang, Y., Wang, C., Risgaard-Petersen, N., Jetten, Mike S M, Yin, C., 2011. Anaerobic ammonia oxidation in a fertilized paddy soil. ISME. 5 (12), 1905–1912.

Zhu, G., Wang, S., Wang, W., Wang, Y., Zhou, L., Jiang, B., Op den Camp, Huub J. M., Risgaard-Petersen, N., Schwark, L., Peng, Y., Hefting, M.M., Jetten, Mike S. M., Yin, C., 2013. Hotspots of anaerobic ammonium oxidation at land–freshwater interfaces. Nature Geosci. 6 (2), 103–107

Appendix – Supplementary Information

Table S1. Main input parameters for the three different PHREEQC models.

PHREEQC		CE Model					CE-Calc Model					CE-Equil-OM-Anammox Model				
Input	Cell	EQ	P1	P2	P3	P4	EQ	P1	P2	P3	P4	EQ	P1	P2	P3	P4
Reactions		Amount added (mmol/L/year)														
$(CH_2O)106(NH_3)16(H_3PO_4)$	1	-	-	-	-	-	-	-	-	-	-	121.9	121.9	121.9	121.9	121.9
(values in mmol C/L/year)	2-7	-	-	-	-	-	-	-	-	-	-	1.06	1.06	1.06	1.06	1.06
	8-42	-	-	-	-	-	-	-	-	-	-	11.66	4.24	4.24	13.78	15.9
$H(NO_3)$[1]	1	-	-	-	-	-	-	-	-	-	-	-	-	-	-	-
	2-42	-	-	-	-	-	-	-	-	-	-	8.54	3.42	2.68	14.52	8.54
O2	1	-	-	-	-	-	-	-	-	-	-	-	-	-	-	-
	2-7	-	-	-	-	-	-	-	-	-	-	6.10	6.10	6.10	6.10	3.05
	8-42	-	-	-	-	-	-	-	-	-	-	3.66	3.66	3.66	3.66	1.22
$Fe(OH)_3$	1	-	-	-	-	-	-	-	-	-	-	9.76	9.76	9.76	9.76	9.76
Equilibrium phases		Saturation index (SI)														
Calcite (4.8 mmol)	1	-	-	-	-	-	0.33	0.33	0.33	0.33	0.33	0.33	0.33	0.33	0.33	0.33
	2-4	-	-	-	-	-	0.25	0.25	0.25	0.25	0.25	0.25	0.25	0.25	0.25	0.25
	5-32	-	-	-	-	-	0.12	0.12	0.12	0.12	0.12	0.12	0.12	0.12	0.12	0.12
	33-42	-	-	-	-	-	0.17	0.17	0.17	0.17	0.17	0.17	0.17	0.17	0.17	0.17
FeS (ppt)	1-42	-	-	-	-	-	-	-	-	-	-	0.00	0.00	0.00	0.00	0.00
CO_2 (g)[2]	1	-	-	-	-	-	-	-	-	-	-	-	-	-	-	-
	2-42	-	-	-	-	-	-	-	-	-	-	-1.6	-1.6	-1.6	-1.6	-1.6

EQ = Input of annual average concentration of GW for 182 steps/1.5 years, P1 = Period from Mar 17-Apr 25 2013: Input of SW Mar '13 for 14 steps/43 days, P2 = Period from Apr 25- May 29 2013: Input of SW Apr '13 for 11 steps/34 days, P3 = Period from May 29-July 22 2013: Input of SW May '13 for 18 steps/53 days, P4 = Period from July 22-Sep 17 2013: Input of SW July '13 for 18 steps/55days, [1] = Derived from oxidation of urea $CO(NH_2)_2$, [2] = Corresponding to P_{CO_2} of 2.5%.

Table S2. Water chemistry of soil water (sampled 0.4, 08, and 1.2 m depth) from March 2013 to March 2014.

Date	**T**	**DO**	**pH**	**HCO_3^-**	**EC***	**Na^+**	**K^+**	**NH_4^+**	**Ca^{2+}**	**Mg^{2+}**	**Cl^-**	**NO_3^-**	**SO_4^{2-}**	**Al^{3+}**	**Fe^{2+}**	**Mn^{2+}**
	˚C	mg/L		meq/L	mS/cm	mmol/L								µmol/L		
$SoilW_{avg}$ 0.4																
13 Apr, 2013	15.0	5.5	7.9	6.4	1.4	5.60	0.03	n.d.	3.09	1.66	3.80	2.96	1.02	0.00	0.14	n.d.
29 May, 2013	23.6	5.3	7.7	14.0	1.8	6.69	0.06	n.d.	4.29	2.57	4.36	n.d.	1.08	n.d.	0.05	0.03
22 Jul, 2013	28.0	6.3	7.6	5.6	1.4	6.68	0.02	0.01	4.14	2.15	4.35	7.02	1.48	n.d.	n.d.	0.07
$SoilW_{avg}$ 0.8																
13 Apr, 2013	15.0	5.4	7.9	7.1	1.3	6.16	0.02	n.d.	2.98	1.86	3.68	2.28	1.41	0.00	0.02	n.d.
22 Jul, 2013	29.6	6.7	7.5	7.3	1.5	5.72	0.08	0.03	3.07	1.75	3.28	2.66	1.40	n.d.	n.d.	0.07
17 Sep, 2013	23.2	5.0	7.5	7.4	1.3	4.86	0.08	0.03	2.83	1.52	3.60	0.17	1.29	1.07	1.51	1.26
$SoilW_{avg}$ 1.2																
12 Mar, 2013	9.1	5.0	7.9	6.5	1.2	4.06	0.01	n.d.	2.53	1.54	3.14	0.28	1.06	0.50	0.07	0.26
13 Apr, 2013	14.9	5.7	7.9	7.5	1.2	4.93	0.02	n.d.	2.60	1.67	3.59	0.22	1.10	3.46	0.30	0.51
29 May, 2013	23.1	5.0	7.7	70.8	1.4	5.41	0.01	0.01	2.73	1.90	4.22	2.37	1.09	n.d.	0.02	0.06
22 Jul, 2013	29.8	5.0	7.8	7.3	1.3	5.25	0.01	0.11	2.52	1.74	2.61	1.64	1.09	n.d.	n.d.	0.19
17 Sep, 2013	23.2	5.3	7.9	7.3	1.2	4.70	0.03	0.10	2.23	1.47	3.05	0.06	1.12	n.d.	0.06	0.64

$SoilW_{avg}$ 0.4 = Average of samples from soil water at 0.4 m depth, $SoilW_{avg}$ 0.8 = Average of samples from soil water at 0.8 m depth, $SoilW_{avg}$ 1.2 = Average of samples from soil water at 1.2 m depth, * = Compensated for 25°C.

Table S3. Percent of carbon dioxide in an atmosphere in equilibrium with the sample and median (top) and range (bottom) of calculated saturation indices different minerals by sample group. The calculation was done via PHREEQC speciation, using measured values of pH, alkalinity and ion concentrations from March 2013 to February 2014.

	RW	HZ	GW1	GW2	GW3	GW4	SoilW
Carbon dioxide (%)	0.54 0.30 to 0.76	1.97 0.54 to 6.58	1.78 0.91 to 3.77	2.71 1.18 to 6.42	2.49 0.88 to 5.00	2.35 0.93 to 4.42	0.71 0.29 to 1.47
Calcite	0.70 0.50 to 1.06	0.33 0.02 to 0.88	0.25 -0.02 to 0.51	0.15 -0.13 to 0.34	0.12 -0.07 to 0.30	0.17 0.01 to 0.28	0.79 0.57 to 1.20
Aragonite	0.54 0.34 to 0.91	0.19 -0.12 to 0.73	0.10 -0.16 to 0.36	0.01 -0.27 to 0.19	-0.04 -0.21 to 0.15	0.01 -0.14 to 0.13	0.64 0.42 to 1.05
Dolomite	1.25 0.68 to 1.99	0.63 0.01 to 1.60	0.28 -0.07 to 0.85	0.03 -0.40 to 0.39	-0.03 -0.34 to 0.25	0.09 -0.15 to 0.32	1.50 1.04 to 2.30
Rhodochrosite	-0.30 -3.21 to 0.08	0.54 0.24 to 0.83	0.38 -1.62 to 0.59	-0.56 -1.22 to -0.19	-0.73 -1.53 to -0.02	-0.59 -3.70 to 0.11	-1.40 -3.37 to -0.16
Siderite	-0.33 -1.05 to 0.14	0.46 -0.43 to 1.02	-0.51 -1.65 to 0.27	-1.07 -1.54 to -0.63	-1.00 -1.87 to -0.02	-0.85 -1.85 to -0.14	-2.07 -3.82 to 0.16
Aluminum hydroxide	-1.45 -4.92 to -0.97	-0.28 -4.28 to 1.17	-3.77 -4.26 to -0.82	-3.67 -4.08 to -0.74	-3.59 -3.94 to -0.29	-3.71 -3.87 to -3.52	-4.44 -4.95 to -0.85
Gibbsite	1.35 -2.26 to 1.87	2.44 -1.61 to 3.97	-0.97 -1.56 to 1.96	-0.88 -1.41 to 2.01	-0.73 -1.23 to 2.47	-0.90 -1.17 to -0.68	-1.78 -2.29 to 1.94
Kaolinite	4.26 -3.19 to 5.88	6.48 -1.31 to 10.74	-0.35 -1.55 to 5.40	-0.43 -1.39 to 5.60	-0.36 -0.96 to 6.64	-0.29 -0.91 to 0.25	-1.77 -2.82 to 6.84
Illite	2.88 -5.48 to 4.93	5.36 -3.69 to 10.41	-3.18 -4.27 to 3.91	-3.75 -4.52 to 3.44	-4.06 -5.01 to 4.54	-4.02 -4.37 to -3.22	-4.52 -6.33 to 5.93
Anorthite	-2.02 -8.24 to -0.60	-0.18 -7.66 to 3.11	-7.77 -8.13 to 1.40	-7.99 -8.41 to -1.68	-8.06 -8.45 to -0.73	-8.04 -8.32 to -7.69	-7.56 -7.92 to 0.60
Montmorillonite	3.02 -5.66 to 5.12	5.80 -3.29 to 11.12	-2.64 -3.83 to 4.16	-2.68 -3.78 to 4.38	-2.81 -3.39 to 5.64	-2.80 -3.29 to -1.98	-3.77 -4.93 to 6.93

RW = River water, HZ = Hyporheic zone, GW = Groundwater, SoilW = Soil water